Low-frequency thermal noise in optical fiber cavities

Scott Foster

Maritime Operations Division, Defence Science and Technology Organisation, Edinburgh, South Australia 5111, Australia

(Received 3 May 2012; published 1 October 2012)

Thermodynamic phase fluctuations in optical fiber cavities are analyzed in detail, with an emphasis on asymptotic behavior in the low-frequency regime. Both exact series solutions and closed-form approximations are derived for thermal noise under a range of different boundary conditions. These results clarify theoretical limits to strain resolution in optical fiber sensors at low frequency, enabling correct interpretation of recent experiments.

DOI: 10.1103/PhysRevA.86.043801 PACS number(s): 42.81.Pa, 42.55.Wd, 42.62.Eh

I. INTRODUCTION

Recently, there has been interest in thermodynamic cavity fluctuations in optical fiber resonators at low frequency [1–6]. Interest in this topic arises from the desire to understand the absolute performance limit of ultrahigh-resolution fiber optic strain sensors [1,7–10]. Such limits may be understood in terms of the fundamental uncertainty in the optical path length of a resonant structure at finite temperature. Thermodynamic cavity fluctuations of similar origin are also believed to impose fundamental limits in related measurement fields, including microresonators [11] and the free-space mirror cavities used for the Laser Interferometric Gravitational Observatory (LIGO) [12–14].

Thermal noise limited phase fluctuations have been observed in fiber-optic interferometers with long interaction lengths (>100 m) over a frequency range from around 1 kHz to 1 MHz [6,15]. Resolving thermal fluctuations in short cavities such as Fabry-Pérot and Bragg grating resonators is more difficult due to the comparatively smaller absolute displacements. Above 100 Hz the most sensitive measurements of cavity fluctuations have been made with distributed feedback (DFB) fiber laser sensors which measure length changes to the resonant cavity of an optical fiber laser by interrogating modulations in laser frequency [7,8]. Above a few kilohertz the measured noise floor is believed to be dominated by fundamental thermal noise [5], yielding an absolute displacement resolution of the order of 10^{-15} mHz$^{-1/2}$ (equivalent to a strain resolution of around 10^{-13} Hz$^{-1/2}$) at 2 kHz for a nominal 1-cm cavity length [8]. At frequencies below 1 kHz, excess (nonequilibrium) thermal fluctuations arising from the pumped active ions are believed to dominate, yielding a $1/f$ thermal noise spectrum at low frequency [4]. While these fluctuations are of fundamental interest in their own right, they are a feature of the active gain medium and limit the capacity of the laser sensor to resolve strain at the true limit imposed by equilibrium thermal fluctuations.

The excess thermal noise in fiber laser sensors has led some authors to argue that passive optical cavities will yield better performance as high-resolution strain sensors at low frequency [9,10]. Although interrogation of passive fiber-optic cavities at the thermal noise limit is yet to be achieved, recent advances suggest that it may soon be possible. By locking a narrow-linewidth laser to a Fabry-Pérot cavity using a sophisticated rf phase modulation technique, the authors of Ref. [9] achieved absolute displacement resolution of better than 10^{-13} mHz$^{-1/2}$ down to approximately 100 Hz and have more recently extended this performance down to frequencies below 10 Hz [10]. Using a refinement of the above technique which stabilized the interrogating laser against an absolute frequency reference, Gagliardi *et al.* [1] recently achieved subpicometer displacement resolution for a Fabry-Pérot cavity in the subhertz frequency domain. They measured a noise floor of about 10^{-13} mHz$^{-1/2}$ Hz at 2 Hz.

These developments provide new opportunities to test our basic understanding of thermal fluctuations; however, considerable care must be exercised in applying the standard theory of thermal noise in the low-frequency domain. Indeed, much of the published theory includes approximations relevant to higher frequencies [4,5,16] and requires modification in order to be applicable at low frequency. It is also far from clear what boundary conditions should apply in situations where the coherence length of thermal fluctuations is large compared to the fiber diameter, such as occurs at very low frequencies. In addition, recent questions have been raised as to the possible role of internal damping in driving thermal noise in fiber [2].

A fiber-optic strain sensor measures changes to the optical path length or transit *phase* of a cavity. Analysis of thermal noise usually begins with the assumption that the optical path length at any instant in time is fully characterized by a set of temperature-dependent material and geometric parameters [4,5,16,17]. More specifically, it is assumed that the change in optical path length in a section of fiber of length L due to a change in temperature ΔT may be written in the form

$$\Delta\phi = nkL\xi\Delta T, \tag{1}$$

where n is the refractive index of the fiber, k is the free-space wave number, and $\xi = n^{-1}dn/dT + \alpha_e$ is an empirical coefficient characterizing the temperature dependence of n and L (α_e is the coefficient of thermal expansion of the fiber). The spectrum of thermally induced phase fluctuations $S_\phi(f)$ may then be written

$$S_\phi(f) = (nkL\xi)^2 S_L(f), \tag{2}$$

where $S_L(f)$ is the power spectral density of temperature fluctuations in a section of fiber of length L. From this point of view, the discussion of thermal noise can be reduced to that of temperature fluctuations in lengths of fiber. Strictly speaking, (1) applies to transitions between equilibrium states. To apply it to fluctuations *about* thermal equilibrium (or pseudoequilibrium in the case of Ref. [4]) requires a careful definition

of ΔT and an implicit assumption that the parameters n and α_e depend only on the instantaneous internal energy of the material within the optical cavity.

An alternative approach to studying thermal noise, widely applied in free-space interferometry [12,14], involves using the fluctuation-dissipation theorem [18] to directly calculate the fluctuation spectra of mechanical degrees of freedom driven by internal dissipation mechanisms (i.e., friction). This approach has recently been applied in the optical fiber domain by Duan [2], who calculated the length fluctuation spectrum of a one-dimensional fiber with complex Young's modulus to obtain a thermomechanical explanation of low-frequency $1/f$ noise.

Note that fluctuations of this type are not equivalent to temperature fluctuations, as may be seen by considering a scenario where the fiber is thermally isolated from the external environment. In that situation, the total energy (and hence temperature) remains constant, but individual mechanical modes fluctuate as they exchange energy with other internal degrees of freedom (via friction). Further insight may be gained by looking at temperature fluctuations from the viewpoint of the fluctuation-dissipation theorem. The temperature (or equivalently energy) can be shown to obey a Langevin equation with dissipation occurring via thermal conduction through the boundary [13], as distinct from thermomechanical fluctuations which are driven by internal damping. To make this distinction explicit, we shall henceforth denote the noise spectra (2) associated with temperature fluctuations as thermoconductive noise. Note that this type of noise is often referred to as thermorefractive noise in the literature [11,13,14].

The current paper is an attempt to clarify the low-frequency thermoconductive theory of thermal noise in an optical fiber and to provide theoretical predictions that may be critically tested against experimental data at frequencies below 100 Hz. In Sec. II we introduce a Green's-function approach which enables an arbitrary uniform boundary condition to be incorporated at the cladding boundary. We derive exact series solutions for the temperature spectrum $S_L(f)$ at thermal equilibrium under both ideal insulating and ideal conducting boundary conditions. In Sec. III we derive approximate closed-form solutions which help clarify the physical interpretation of the spectrum, and in Sec. IV we examine asymptotic power-law behavior in the low-frequency limit. In Sec. V the theory is extended to active (laser) cavities, where an additional "$1/f$" contribution needs to be added to account for nonequilibrium processes. We conclude with a discussion in Sec. VI.

II. THE EQUILIBRIUM THERMAL FLUCTUATION SPECTRUM

We define the instantaneous temperature T by the relation $T = u/c_v$, where u is the internal energy per unit volume and c_v is the specific heat. In this way we may identify energy fluctuations at thermal equilibrium with instantaneous temperature fluctuations.

To calculate the spectrum of temperature fluctuations in an optical fiber at thermal equilibrium we begin with the inhomogeneous heat equation [19]

$$\nabla^2 T - \frac{c_v}{\kappa_t}\dot{T} = \frac{\boldsymbol{\nabla}\cdot\boldsymbol{h}}{\kappa_t}, \tag{3}$$

where κ_t is the coefficient of thermal conductivity and $\boldsymbol{h}$ is a random heat current (the so-called Langevin source) which acts as a source of energy fluctuations within a given material element. We shall assume that the material parameters c_v and κ_t are uniform throughout the fiber. Strictly speaking, the fiber core and cladding have slightly different material properties due to the presence of index-modifying dopants in the core; however, it is reasonable to assume that these dopants make a negligible contribution to thermal diffusion.

Rather than solving (3) directly, we shall begin by calculating a Green's function $G(t,\boldsymbol{r},\boldsymbol{r}')$. This will enable appropriate boundary conditions to be incorporated. Thus we consider the equation

$$\nabla^2 G - \frac{c_v}{\kappa_t}\dot{G} = -\delta(t)\delta^3(\boldsymbol{r}-\boldsymbol{r}'). \tag{4}$$

Taking the Fourier transform with respect to the time coordinate gives

$$(\nabla^2 - i\tilde{k}^2)G(\omega,\boldsymbol{r},\boldsymbol{r}') = -(2\pi)^{-1}\delta^3(\boldsymbol{r}-\boldsymbol{r}'), \tag{5}$$

where $\tilde{k} = \sqrt{c_v\omega/\kappa_t}$ and ω is the (angular) frequency. It is also convenient to decompose the ∇^2 operator into its axial and tangential parts, $\nabla^2 = \nabla_\perp^2 + \nabla_z^2$, where

$$\nabla_\perp^2 = \frac{\partial^2}{\partial x^2} + \frac{\partial^2}{\partial y^2}, \tag{6a}$$

$$\nabla_z^2 = \frac{\partial^2}{\partial z^2}. \tag{6b}$$

We assume an infinitely long, uniform cylindrical fiber of radius R; then the solution may be expressed in terms of the infinite series expansion:

$$G = \sum_{m,l} \psi_{lm}(r,\theta) f_{lm}(z,\boldsymbol{r}'), \tag{7}$$

where m and l are non-negative integers and ψ_{lm} constitute a complete orthonormal set of eigenfunctions satisfying the eigenvalue equation

$$(\nabla_\perp^2 + k_{lm}^2)\psi = 0 \tag{8}$$

along with an appropriate boundary condition at $r = R$. The orthonormality condition may be expressed as

$$\int_0^R \int_0^{2\pi} r\psi_{lm}\psi_{l'm'}\,dr\,d\theta = \delta_{ll'}\delta_{mm'}. \tag{9}$$

Substituting Eqs. (7) into (5), multiplying by ψ_{lm}, and integrating over the fiber cross section give

$$\left(\nabla_z^2 - p_{lm}^2\right) f_{lm} = -(2\pi)^{-1}\psi_{lm}(r',\theta')\delta(z-z'), \tag{10}$$

where $p_{lm} = \sqrt{i\tilde{k}^2 + k_{lm}^2}$. Thus, in terms of the axial wavenumber (Fourier space) representation,

$$f_{lm}(k_z,\boldsymbol{r}') = \psi_{lm}(r',\theta')g_{lm}(k_z,z'), \tag{11}$$

where

$$g_{lm} = \frac{e^{-ik_z z'}}{(2\pi)^2\left(k_z^2 + p_{lm}^2\right)}, \tag{12}$$

or, taking the inverse Fourier transform with the help of Cauchy's residue theorem,

$$g_{lm}(z-z') = \frac{e^{-p_{lm}|z-z'|}}{4\pi p_{lm}}. \tag{13}$$

Note from Eqs. (7) and (11) the important symmetry relation $G(\omega,\boldsymbol{r},\boldsymbol{r}') = G(\omega,\boldsymbol{r}',\boldsymbol{r})$.

It remains to solve (8) to obtain the eigenvalues k_{lm} and eigenfunctions $\psi_{lm}(r,\theta)$. The general solution to the two-dimensional Helmholtz equation (8) with radial boundary conditions is

$$\psi_{lm}(r,\theta) = A_{lm} J_l(k_{lm} r)\cos[l(\theta+\theta_0)], \tag{14}$$

where θ_0 is an arbitrary constant, J_l are the Bessel functions of order l [20], and the eigenvalues k_{lm} and normalization coefficients A_{lm} are determined by the appropriate boundary conditions. For example, if ideal conductive boundary conditions are imposed at $r = R$, then we have $\psi_{lm}(R,\theta) = 0$, which yields the transcendental equation for k_{lm},

$$J_l(k_{lm} R) = 0, \tag{15a}$$

for which the normalization constraint yields

$$A_{lm} = \frac{\epsilon_l}{\sqrt{\pi} R J_l'(k_{lm} R)}, \tag{15b}$$

where ϵ_l equals 1 for $l = 0$ and $\sqrt{2}$ for $l > 0$. Note that (15a) defines an infinite number of solutions for any given l (one for each value of the m index), with successively larger solutions corresponding to successive values of m. The index l may be thought of as the angular mode number, while m labels radial modes.

Similarly, insulating boundary conditions (vanishing heat flow at the boundary) yield

$$J_l'(k_{lm} R) = 0 \tag{16a}$$

$$A_{lm} = \frac{\epsilon_l k_{lm}}{\sqrt{\pi}\left(k_{lm}^2 R^2 - l^2\right)^{\frac{1}{2}} J_l(k_{lm} R)}. \tag{16b}$$

Insulating and conducting boundary conditions might be considered two ideals which represent the extremes of thermal behavior at the boundary, and we shall focus on these cases below. Another important case, which has proven useful for generating exact solutions, occurs when the thermal properties of the external material are perfectly matched to that of the cladding. Since the boundary becomes invisible to the thermal fluctuation, this is equivalent to an infinitely thick cladding; i.e., $R \to \infty$.

Having calculated the correct Green's function, the solution to Eq. (3) may now be expressed (in the frequency domain) as

$$T(\omega,\boldsymbol{r}) = \frac{-2\pi}{\kappa_t}\int G(\omega,\boldsymbol{r},\boldsymbol{q})\nabla_q \cdot \boldsymbol{h}(\omega,\boldsymbol{q}) d^3q, \tag{17}$$

where the integral is taken over the extent of the fiber and the ∇_q operator acts on functions of $\boldsymbol{q} = (q_x,q_y,q_z)$. Integrating by parts and ignoring the boundary term (which vanishes identically under ideal insulating or conducting conditions) yields the more convenient expression

$$T(\omega,\boldsymbol{r}) = \frac{2\pi}{\kappa_t}\int \nabla_q G(\omega,\boldsymbol{r},\boldsymbol{q}) \cdot \boldsymbol{h}(\omega,\boldsymbol{q}) d^3q. \tag{18}$$

Our objective is to calculate the correlation function of T. To do this we make use of the following result from the theory of fluctuations [19]:

$$\langle h_i(\omega,\boldsymbol{r}) h_j^*(\omega',\boldsymbol{r}')\rangle = \frac{\kappa_t K T^2}{\pi}\delta_{ij}\delta(\omega-\omega')\delta^3(\boldsymbol{r}-\boldsymbol{r}'), \tag{19}$$

where K is Boltzmann's constant, from which it easily follows that

$$\langle T(\omega,\boldsymbol{r}) T^*(\omega',\boldsymbol{r}')\rangle = \frac{4\pi K T^2}{\kappa_t}\delta(\omega-\omega')F(\omega,\boldsymbol{r},\boldsymbol{r}'), \tag{20}$$

where

$$F(\omega,\boldsymbol{r},\boldsymbol{r}') = \int \nabla_q G(\boldsymbol{r},\boldsymbol{q}) \cdot \nabla_q G^*(\boldsymbol{r}',\boldsymbol{q}) d^3q \tag{21}$$

$$= (2\pi)^{-1} G(\boldsymbol{r},\boldsymbol{r}') + i\tilde{k}^2 \int G(\boldsymbol{q},\boldsymbol{r}) G^*(\boldsymbol{q},\boldsymbol{r}') d^3q, \tag{22}$$

where the frequency dependence of G has been suppressed for notational convenience. Equation (22) was obtained from Eq. (21) using integration by parts to obtain a $\nabla^2 G^*$ term in the integrand (and a boundary term which shall be equated to zero), followed by substitution of the complex conjugate of Eq. (5). Now, it is intuitively obvious (and may readily be shown) that F should be symmetric with respect to the interchange of $\boldsymbol{r}$ and $\boldsymbol{r}'$. Using this fact, it follows from Eq. (21) that F is real. Taking the real part of Eq. (22) and making use again of the symmetry with respect to $\boldsymbol{r}$ and $\boldsymbol{r}'$ and of the fact that $\tilde{k}^2$ is real, we obtain a remarkable simplification:

$$F(\omega,\boldsymbol{r},\boldsymbol{r}') = (2\pi)^{-1}\mathrm{Re}[G(\boldsymbol{r},\boldsymbol{r}')]. \tag{23}$$

The solution may be expressed explicitly in terms of the orthonormal basis:

$$F = (2\pi)^{-1}\sum_{lm}\psi_{lm}(r,\theta)\psi_{lm}(r',\theta')\mathrm{Re}[g_{lm}(z-z')]. \tag{24}$$

The instantaneous temperature $T(\omega,\boldsymbol{r})$ at each point $\boldsymbol{r}$ is defined in terms of local fluctuations in energy density at that point. The instantaneous temperature of a finite section of fiber is derived by averaging over the mode volume. From Eq. (20) we obtain, for a section of fiber of length L,

$$\langle T(\omega) T^*(\omega')\rangle_L = \frac{4\pi K T^2}{\kappa_t L}\delta(\omega-\omega')\tilde{F}(\omega), \tag{25}$$

where

$$\tilde{F}(\omega) = L^{-1}\int rr' M(r)^2 M(r')^2 F(\omega,\boldsymbol{r},\boldsymbol{r}') dr dr' d\theta d\theta' dz dz', \tag{26}$$

where $M(r)$ is the mode-amplitude profile. This integral includes a z-dependent part,

$$L^{-1}\int_0^L\int_0^L dz dz' \mathrm{Re}[g_{lm}(z-z')]$$

$$= \mathrm{Re}\left[\frac{1}{2\pi p_{lm}^2}\left(1 - \frac{(1-e^{-p_{lm}L})}{L p_{lm}}\right)\right]. \tag{27}$$

The last term in brackets is a boundary term of order $(p_{lm}L)^{-1}$. This term may usually be considered small; however, we note that for the special case of insulating boundary conditions

$k_{00} = 0$, which gives $p_{00} \propto \tilde{k}$. In this case and *only* this case, the boundary term diverges as $\omega^{-1/2}$ in the low-frequency limit. Ignoring this pathological situation for the moment, we shall assume that the boundary term is small and may be ignored to leading order, yielding, upon integration of Eq. (26),

$$\tilde{F}(\omega) = \frac{1}{4\pi^2} \sum_m \Psi_m^2 \frac{k_{0m}^2}{\left(\tilde{k}^4 + k_{0m}^4\right)}, \tag{28}$$

where

$$\Psi_m = \int r M(r)^2 \psi_{0m}(r,\theta) dr d\theta. \tag{29}$$

Note that, as would be expected for a uniformly distributed heat source, all the higher-order angular modes dropped out due to their periodicity with respect to θ. Let us assume a Gaussian profile $M^2 \simeq 2\exp(-2r^2/a^2)/\pi a^2$, where a is the *mode radius*; then Ψ_m may be evaluated exactly:

$$\Psi_m^2 = A_{m0}^2 e^{-k_{0m}^2 a^2/4}. \tag{30}$$

Substituting Eqs. (30) into (28) and using the explicit mode-amplitude expressions (15) and (16) for conducting and insulating boundary conditions, respectively, noting the identity $J_0'(x) = -J_1(x)$, we obtain the general expression

$$\tilde{F}(\omega) = \sum_m \frac{k_m^2 e^{-k_m^2 a^2/4}}{4\pi^3 R^2 J_\nu^2(k_m R)\left(\tilde{k}^4 + k_m^4\right)}, \tag{31}$$

where we have introduced the abbreviated notation $k_m = k_{0m}$ and ν equals 0 or 1 for insulating or conducting boundary conditions, respectively. The modal wave numbers k_m satisfy the appropriate algebraic constraint (15a) or (16a).

To complete the calculation we need to relate the frequency domain correlation function (25) to the power spectral density. For any stationary process α with correlation function of the form $\langle \alpha(\omega)\alpha^*(\omega')\rangle = F(\omega)\delta(\omega - \omega')$ the two-sided power spectral density $S_\alpha(f)$ may be *defined* as 2π times the argument of the δ function [21]. By inspection of Eq. (25) we thus have

$$S_L(f) = \frac{8\pi^2 K T^2}{\kappa_t L} \tilde{F}(2\pi f), \tag{32}$$

where $f = \omega/2\pi$ and $\tilde{F}$ is given by Eq. (31). Figure 1 shows the theoretical phase fluctuation spectrum of a 1-m fiber from 0.1 Hz to 10 kHz with insulating, conducting, and infinite-cladding conditions. The infinite cladding case was calculated using the formulas derived in Ref. [5]. The insulating boundary condition curve agrees with the commonly applied Wanser theory [17] to within 1 dB. The fiber parameters used in the calculations are shown in Table I.

Observe that the dependence on boundary conditions is relatively weak overall. Note also that for frequencies above about 200 Hz the spectrum is completely insensitive to boundary conditions. This may be heuristically understood as follows: From Eq. (5) we expect the correlation length of thermal fluctuations to be roughly equal to the inverse of $\tilde{k}$,

$$L_c \sim \tilde{k}^{-1} = \frac{3.6 \times 10^{-4}}{\sqrt{f}}.$$

Thus at 200 Hz we get $L_c \sim 25\ \mu$m, which is roughly half the cladding radius. At higher frequencies most fluctuations decay before reaching the cladding boundary and therefore never "see" the boundary conditions. At low frequencies the correlation length becomes comparable to, or greater than, the cladding diameter, which is why boundary conditions become important in this domain. Although all this is intuitively obvious, it is not transparent from Eq. (31). It is also far from obvious that letting R tend to infinity in Eq. (31) will give an equivalent result to the infinite-cladding case derived in Ref. [5] (it does). It is worth examining this expression more closely, as will be done in the next section.

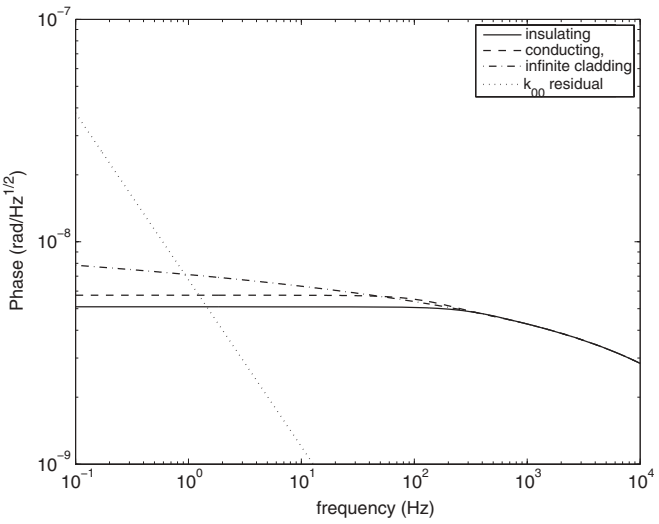

FIG. 1. Theoretical rms phase fluctuation spectra at thermal equilibrium assuming insulating (solid curve), conducting (dashed curve), and infinite-cladding (dot-dashed curve) boundary conditions. The dashed curve is the residual contribution from the k_{00} mode with insulating boundary conditions derived in Sec. IV.

III. CLOSED-FORM APPROXIMATIONS TO $\tilde{F}$

Let $z_m^{(0)}$ and $z_m^{(1)}$ be the $(m+1)$th zeros of $J_0'(z)$ and $J_0(z)$, respectively. Then $k_m = z_m^{(\nu)}/R$, and we may rewrite (31) in the form

$$\tilde{F}(\omega) = \sum_m \frac{z_m^{(\nu)2} e^{-z_m^{(\nu)2} a^2/4R^2}}{4\pi^3 J_\nu^2\left(z_m^{(\nu)}\right)\left(R^4\tilde{k}^4 + z_m^{(\nu)4}\right)}. \tag{33}$$

TABLE I. Fiber parameters used in calculations.

Symbol	Name	Value
a	mode field radius	2.5 μm
R	cladding radius	62.5 μm
L	fiber length	1 cm
n	refractive index	1.457
k	wave number	6.6×10^3 cm^{-1}
ξ	thermo-optic coefficient	7×10^{-6} K^{-1}
T	temperature	293 K
K	Boltzmann's constant	13.81×10^{-24} J K^{-1}
c_v	specific heat of silica	1.67×10^6 J m^{-3} K^{-1}
κ_t	thermal conductivity of silica	1.37 W (mK)$^{-1}$
Q	non-Langevin source strength	8.3×10^{-8} J^2 m^{-3} s^{-1}

It becomes apparent that $\tilde{F}$ is determined by just two dimensionless parameters: $\tilde{k}R \equiv R/L_c$ and R/a. For the case of insulating boundary conditions ($\nu = 0$), the first zero is at the origin (i.e., $z_0^{(0)} = 0$). If follows from Eq. (33) that this mode makes no contribution to $\tilde{F}$ [Recalling the discussion immediately following (27) this should raise concerns, but we shall press on for now]. The first nontrivial zero is $z_1^{(0)} = 3.83$ and for $m > 1$ we may apply the asymptotic approximation $z_m^{(0)} \simeq \pi(m + 1/4)$. Similarly, for conducting boundary conditions we have $z_m^{(1)} \simeq \pi(m + 3/4)$ for $m > 0$. Also, for $m > 1$, $J_\nu(z_m^{(\nu)}) \simeq \pm\sqrt{2/\pi z_m^{(\nu)}}$ [20]. Thus we may write

$$\tilde{F}(\omega) \simeq \frac{z_1^{(\nu)2} e^{-z_1^{(\nu)2}a^2/4R^2}}{4\pi^3 J_\nu^2(z_1^{(\nu)})(R^4\tilde{k}^4 + z_1^{(\nu)4})} + \sum_{m=2}^{\infty} \mathrm{Re}\left[\frac{m e^{-\pi^2 m^2 a^2/4R^2}}{8\pi(R^2 i\tilde{k}^2 + \pi^2 m^2)}\right], \tag{34}$$

where we have expanded each element of the infinite sum into its complex factors and have changed the labeling convention slightly to denote by $z_1^{(\nu)}$ the first *nontrivial* zero. Notice that the details of the boundary conditions reside entirely within the first term. The rest of the expression depends on the boundary through the cladding radius R but is insensitive to the specific boundary conditions. Rather than evaluating this sum exactly, we approximate it by a continuous integral [22]; i.e., we write $\tilde{F} = F_1 + F_\infty$, where F_1 is the first term in Eq. (34) and

$$F_\infty \simeq \pi^{-3}\mathrm{Re}\left[\int_{\xi=\pi a/R}^{\infty} \frac{\xi e^{-\xi^2}}{2(a^2 i\tilde{k}^2 + 4\xi^2)} d\xi\right] = \frac{1}{16\pi^3}\mathrm{Re}\left[e^{ia^2\tilde{k}^2/4} E_1\left(\frac{\pi^2 a^2}{R^2} + \frac{ia^2\tilde{k}^2}{4}\right)\right], \tag{35}$$

where E_1 is the exponential integral function [20]. This expression tells us everything we need to know. First, in the limit $R \to \infty$ the R-dependent term vanishes, and the resulting expression is identical to the spectrum derived in Ref. [5] under the infinite-cladding conditions. As was shown in that paper, the expression simplifies significantly in the low-frequency regime, and we get

$$\tilde{F} \simeq F_1 - \frac{1}{32\pi^3}\ln\left(\frac{\pi^4 a^4}{R^4} + \frac{a^4\tilde{k}^4}{16}\right) - \gamma, \tag{36}$$

where $\gamma = 0.577$ is Euler's constant. From this, we can readily see that the necessary condition for the boundary to influence the thermal spectrum is $\tilde{k}R < 2\pi$, which confirms our earlier heuristic result.

IV. THE k_{00} MODE WITH INSULATING BOUNDARY CONDITIONS

It has already been noted that the first zero of J_0' equals zero, and thus, according to Eq. (31), the k_{00} mode with insulating boundary conditions makes no contribution to the thermal spectrum. However, from (13) the corresponding Green's function G_{00} diverges as $1/\tilde{k}_{lm} \sim 1/\sqrt{f}$ in the low-frequency limit. It consequently follows from Eqs. (20) and (23) that the k_{00} mode *dominates* the thermal correlation function at low frequency. Indeed in the low-frequency limit

$$\langle T(\omega,\boldsymbol{r})T^*(\omega',\boldsymbol{r}')\rangle \simeq \frac{4\pi K T^2}{\kappa_t}\delta(\omega-\omega')F(\omega,|z-z'|), \tag{37}$$

where

$$F(\omega,r) = \frac{e^{-\tilde{k}r/\sqrt{2}}\cos(\tilde{k}r/\sqrt{2} + \pi/4)}{8\pi^3 R^2\tilde{k}}, \tag{38}$$

which diverges in the limit as $1/\sqrt{f}$. It seems remarkable that the mode that dominates the local thermal fluctuations does not even appear in the spectral density. The solution to this apparent anomaly lies in the integral over $z - z'$ (27). Since the leading-order term vanishes by virtue of p_{lm}^2 being purely imaginary, we can no longer ignore the boundary term, which gives a residual nonzero contribution,

$$\tilde{F}_{00} = \frac{1 - \sqrt{2}e^{-\tilde{k}L/\sqrt{2}}\cos(\tilde{k}L/\sqrt{2} - \pi/4)}{4\sqrt{2}\pi^3 L R^2\tilde{k}^3}, \tag{39}$$

which must be added to $\tilde{F}$ in Eq. (32) to obtain the correct spectrum at sufficiently low frequency. Note that this term only applies for the case of ideal insulating boundary conditions since these are the only boundary conditions that support a zero eigenvalue mode $k_{00} = 0$. Physically, this mode corresponds to pure one-dimensional diffusion of heat along the z axis. Thus, no heat diffuses across the boundary at $r = R$. As soon as diffusion through the boundary (conduction) is allowed, this mode is eliminated.

Letting $\tilde{k}L \to 0$, we obtain the asymptotic expression

$$\tilde{F}_{00}|_{kL\ll 1} = \frac{L}{8\sqrt{2}\pi^3 R^2\tilde{k}}, \tag{40}$$

which diverges as $1/\sqrt{f}$. Equation (40) is equivalent to the thermoconductive noise spectrum previously derived for dielectric mirror coatings [13]. In this regime, thermal fluctuations are correlated over the entire cavity and the temperature may be considered uniform within the cavity. Physically, this can be understood as the adiabatic regime where the rate of change of the total energy is slow compared to the internal diffusion rate. The cavity passes through a succession of quasiequilibrium states as thermal energy is exchanged with neighboring fiber sections. It is perhaps worth observing that this is the only regime where the empirical relation (1) may be applied in its strict quasistatic sense (notwithstanding the fact that the thermoconductive theory is well established experimentally at higher frequencies [6,15,23]).

For a 1-cm cavity, $\tilde{k}L < 1$ corresponds to $f < 10^{-3}$ Hz, so the asymptotic behavior (40) is not really observable even for very short cavities. At all measurable frequencies $\tilde{k}L \gg 1$, and we may use the simplified expression for $\tilde{F}_{00}$:

$$\tilde{F}_{00} = \frac{1}{4\sqrt{2}\pi^3 L R^2\tilde{k}^3}, \tag{41}$$

which goes as $f^{-3/2}$. In this regime, the correlation length is small compared to L but still large compared to R. Since $\tilde{k}^{-1} \ll 1$ at measurable frequencies, $\tilde{F}_{00}$ may generally be expected to be a small correction. From Fig. 1 it may be seen that for the parameters in Table I $\tilde{F}_{00}$ is not measurable above 2 Hz; however, by 0.5 Hz it results in a noise excess of approximately 3 dB.

V. EXCESS NOISE IN LASER CAVITIES

Our calculations so far have dealt with thermal fluctuations under conditions of thermal equilibrium. The situation in "active" laser cavities is somewhat more complicated due to the presence of nonequilibrium processes. Experimentally, it has been established that thermal noise in laser cavities exceeds the equilibrium thermodynamic limit at frequencies below a few kilohertz, where it is dominated by an approximate $1/f$ spectrum [23,24]. To understand this phenomenon we add an additional source term to the classical diffusion equation [4]:

$$\nabla^2 T - \frac{c_v}{\kappa_t}\dot{T} = \frac{\nabla\cdot\boldsymbol{h}}{\kappa_t} - \frac{j}{\kappa_t}, \tag{42}$$

where the non-Langevin source j represents random fluctuations in the rate of heat production per unit volume *within* the material. It has been proposed that these fluctuations arise from minute entropy changes that occur during spontaneous emission events in the excited gain medium [4]. Like $\boldsymbol{h}$, j is assumed to be uncorrelated in space and time:

$$\langle j(\omega,\boldsymbol{r})j^*(\omega',\boldsymbol{r}')\rangle = \frac{Q}{2\pi}\delta(\omega-\omega')\delta^3(\boldsymbol{r}-\boldsymbol{r}') \tag{43}$$

for some temperature-dependent source strength Q. The value of Q used in our calculations (see Table I) is estimated empirically from measurements of $1/f$ frequency noise in DFB fiber lasers. In Ref. [4] it is argued that $Q \propto (KTN)^2$, where N is the density of active ions.

If we write the total temperature fluctuation as $T = T_e + T_a$, where T_e is the "equilibrium" fluctuation resulting from $\boldsymbol{h}$ and T_a is the active fluctuation due to j, then, proceeding in the same way we did for the Langevin source, we may construct T_a from the Green's function:

$$T_a(\omega,\boldsymbol{r}) = \frac{2\pi}{\kappa_t}\int G(\omega,\boldsymbol{r},\boldsymbol{q})j(\omega,\boldsymbol{q})d^3q, \tag{44}$$

where the subscript a stands for active. Taking the correlation function, using (43),

$$\langle T_a(\omega,\boldsymbol{r})T_a^*(\omega',\boldsymbol{r}')\rangle = \frac{2\pi Q}{\kappa_t^2}\delta(\omega-\omega')F_a(\omega,\boldsymbol{r},\boldsymbol{r}'), \tag{45}$$

where

$$F_a(\omega,\boldsymbol{r},\boldsymbol{r}') = \int G(\boldsymbol{r},\boldsymbol{q})G^*(\boldsymbol{r}',\boldsymbol{q})d^3q \tag{46}$$

$$= -(2\pi)^{-1}\mathrm{Im}\left(\frac{G(\boldsymbol{r},\boldsymbol{r}')}{\tilde{k}^2}\right). \tag{47}$$

Integrating over the spatial variables, we get, once again,

$$\langle T_a(\omega)T_a^*(\omega')\rangle_L = \frac{2\pi Q}{\kappa_t^2 L}\delta(\omega-\omega')\tilde{F}_a(\omega), \tag{48}$$

where

$$\tilde{F}_a(\omega) = \sum_m \frac{e^{-k_m^2 a^2/4}}{4\pi^3 R^2 J_\nu^2(k_m R)\left(\tilde{k}^4 + k_m^4\right)}. \tag{49}$$

Note the key difference between this expression and (31) is the absence of the k_m term in the numerator. As a consequence the low-order modes make a proportionally larger contribution. (In particular, for insulating boundary conditions, the $k_{00} = 0$ mode contributes a nonzero term, leading to a $1/f^2$ divergence at low frequency.)

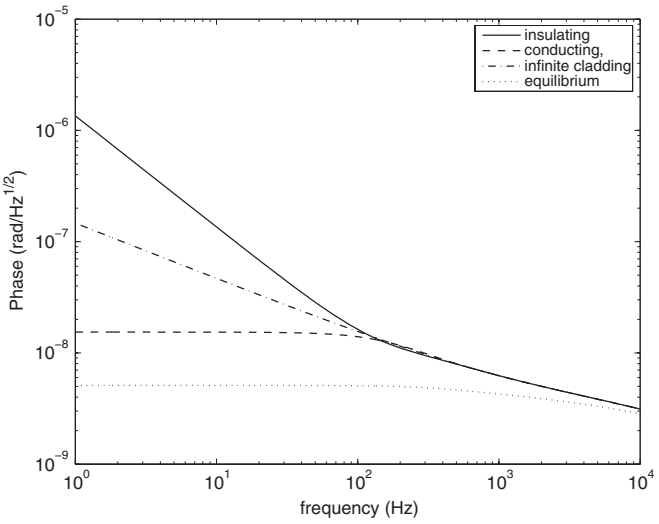

FIG. 2. Theoretical rms phase fluctuation spectra for an active fiber, assuming insulating (solid curve), conducting (dashed curve), and infinite-cladding (dot-dashed curve) boundary conditions. The dashed curve shows the thermal noise limit under equilibrium conditions (with insulating boundary).

If we relabel our original $\tilde{F}$ from Eq. (31) as $\tilde{F}_e$, the modified expression for the thermal fluctuation spectrum becomes

$$S_L(f) = \frac{8\pi^2 KT^2}{\kappa_t L}\tilde{F}_e(2\pi f) + \frac{4\pi^2 Q}{\kappa_t^2 L}\delta(\omega-\omega')\tilde{F}_a(2\pi f). \tag{50}$$

Corresponding phase fluctuation spectrums for insulating, conducting, and infinite-cladding boundary conditions are shown in Fig. 2. Heuristically, the dramatic difference between conducting and insulating boundary conditions is not surprising: Since the fluctuations arise from excess heat generated within the fiber core, efficient transport of heat away from the fiber reduces their influence. As with equilibrium fluctuations, the various regimes of behavior are most transparent via an analytic approximation. Using the same approach as in Sec. III we may write

$$\tilde{F}_a = F_{a0} + F_{a1} + F_{a\infty}, \tag{51}$$

where

$$F_{a0} = \frac{(1-\nu)}{4\pi^3 R^2 \tilde{k}^4} \tag{52}$$

is the $1/f^2$ divergence, which manifests for *insulating conditions* ($\nu = 0$) *only*,

$$F_{a1} = \frac{R^2 e^{-z_1^{(\nu)2}a^2/4R^2}}{4\pi^3 J_\nu^2\left(z_1^{(\nu)}\right)\left(R^4\tilde{k}^4 + z_1^{(\nu)4}\right)} \tag{53}$$

is the lowest-order *finite* term in the infinite series (49), and

$$F_{a\infty} \simeq -\frac{1}{16\pi^3\tilde{k}^2}\mathrm{Im}\left[e^{ia^2\tilde{k}^2/4}E_1\left(\frac{\pi^2 a^2}{R^2} + \frac{ia^2\tilde{k}^2}{4}\right)\right]. \tag{54}$$

At low frequency ($\tilde{k}a \ll 1$) this expression simplifies to

$$F_{a\infty} \simeq \frac{1}{16\pi^3\tilde{k}^2} \arctan\left(\frac{\tilde{k}^2R^2}{4\pi^2}\right), \tag{55}$$

which in turn has two distinct regimes: For $\tilde{k}R > 2\pi$ the arctan function returns $\pi/2$ and $F_{a\infty} \simeq 1/(32\pi^2\tilde{k}^2)$, corresponding to the classic $1/f$ behavior frequently observed in laser frequency noise. This also accounts for the true $1/f$ behavior exhibited by infinite cladding ($R = \infty$) solutions [4]. For $\tilde{k}R \ll 1$, $F_{a\infty}$ approaches a finite limit

$$F_{a\infty} \simeq \frac{R^2}{64\pi^5}.$$

Note that this limiting value has a strong (R^2) dependence on the fiber diameter. This should be compared to the much weaker $\ln R$ dependence on fiber diameter in Eq. (36). This observation leads to a remarkable conclusion: By reducing the diameter of the fiber by just a small amount, it is theoretically possible to push the non-Langevin thermal noise level below that of the conventional thermal noise. In other words, fiber lasers can, in principle, achieve the absolute limit of resolution imposed by equilibrium fluctuations.

VI. DISCUSSION

A comprehensive theoretical analysis of fundamental thermoconductive fluctuations in both passive and active optical fiber cavities has been carried out. In particular, we have clarified the low-frequency thermodynamic limits to cavity phase measurements and have found analytic solutions for simple boundary conditions at the fiber-cladding interface including both conducting and insulating conditions. In the case of insulating boundary conditions the predicted equilibrium spectrum agrees with the commonly used Wanser thermal noise limit [17] to within 1 dB so long as one ignores the residual effect of the $k_{00} = 0$ mode. However, from Eq. (41), this effect can become significant at very low frequencies (below 2 Hz) and may be observable under certain conditions.

Perhaps the most interesting result is the strong dependence of excess noise in active cavities on thermal boundary conditions. It is generally believed that the thermal noise in laser cavities exceeds that of a passive cavity by greater than 20 dB at 10 Hz. However, Fig. 2 shows that with ideal conducting boundary conditions the theoretical noise converges to a finite limit, which, for a standard single-mode fiber with a cladding radius of 62.5 μm, exceeds the equilibrium thermal noise limit by only a factor of 2. Furthermore, the smaller the cladding diameter is, the lower the nonequilibrium noise is. For a cladding radius of 25 μm the equilibrium and nonequilibrium contributions are essentially equal.

From the phase spectral density (2) it is straightforward to infer an equivalent strain spectral density from the relationship $\phi \simeq 0.8nkL\epsilon$, where ϵ is strain and the factor of 0.8 arises due to the strain-optic coefficient. For a 130-mm-long cavity such as that used in Ref. [1], the theoretical thermal noise-limited strain resolution is 2×10^{-14} Hz$^{-1/2}$ at 5 Hz. Note that this figure is much lower than the measured noise floor of approximately 10^{-12} Hz$^{-1/2}$ reported in Ref. [1], which was claimed to represent the thermal noise limit. Detailed objections to this claim have been reported elsewhere [6,25]. We note here that our analysis confirms that the resolution reported in Ref. [1] did not approach the limit imposed by equilibrium (thermoconductive) fluctuations.

It is noteworthy that (40) predicts a power law divergence in low frequency thermal noise for a passive resonator with insulating boundary conditions. Thus, it is not strictly necessary to invoke a thermomechanical explanation for $1/f^n$ noise in passive optical fiber cavities [2]. $1/f^n$ fluctuations may be viewed as a natural feature of one-dimensional dissipative systems. Temperature fluctuations become effectively one-dimensional only when the correlation length $\tilde{k}^{-1}$ is large compared to the largest relevant dimension of the resonator (in this case L). Therefore (40) only becomes manifest at extremely low frequencies ($<10^{-2}$ Hz). The fluctuation-dissipation approach followed in Ref. [2] provides a means of systematically investigating fluctuations of individual degrees of freedom, thereby yielding $1/f$ spectra that might conceivably dominate in some frequency ranges depending on the magnitude of the relevant frictional coefficient (loss angle). For the LIGO (free-space) mirror cavities the various dissipation mechanisms contributing to thermal noise have been systematically investigated from this standpoint, and the relative importance of different noise components in various frequency regimes is believed to be well understood [14]. For optical fibers, the respective roles of thermomechanical and thermoconductive fluctuations at frequencies below 1 kHz remain an open question [6]. Measurements of temperature dependence of $1/f$ noise in DFB fiber lasers in the range from 10 Hz to 100 kHz [23] indicate that $S_\phi \propto T^2$, which is not consistent with thermomechanical noise. Thus, at least for active cavities the existing evidence suggests that thermoconductive effects dominate.

[1] G. Gagliardi, M. Salza, S. Avino, P. Ferraro, and P. D. Natale, Science **330**, 1081 (2010).
[2] L. Duan, Electron. Lett. **46**, 1515 (2010).
[3] G. Cranch and G. Miller, Opt. Lett. **36**, 906 (2011).
[4] S. Foster, Phys. Rev. A **78**, 013820 (2008).
[5] S. Foster, A. Tikhomirov, and M. Milnes, IEEE J. Quantum Electron. **43**, 378 (2007).
[6] R. Bartolo, A. Tveten, and A. Dandridge, IEEE J. Quantum Electron. **48**, 720 (2012).
[7] K. Koo and A. Kersey, Electron. Lett. **31**, 1180 (1995).
[8] G. A. Cranch, G. M. H. Flockhart, and C. K. Kirkendall, IEEE Sens. J. **8**, 1161 (2008).
[9] J. Chow, I. Littler, G. de Vine, D. McClelland, and M. Gray, J. Lightwave. Technol. **23**, 1881 (2005).
[10] I. Littler, M. Gray, J. Chow, D. Shaddock, and D. McClellend, Opt. Express **17**, 11077 (2010).
[11] M. Gorodetsky and I. Grudinin, J. Opt. Soc. Am. B **21**, 697 (2004).
[12] Y. Levin, Phys. Rev. D **57**, 659 (1998).
[13] Y. Levin, Phys. Lett. A **372**, 1941 (2008).

[14] S. Rao, Ph.D. thesis, California Institute of Technology, 2003.
[15] K. H. Wanser, A. Kersey, and A. Dandridge, Opt. Photonics News **4**, 37 (1993).
[16] W. Glenn, IEEE J. Quantum Electron. **25**, 1218 (1989).
[17] K. H. Wanser, Electron. Lett. **28**, 53 (1992).
[18] F. Reif, *Fundamentals of Statistical and Thermal Physics* (McGraw-Hill International Editions, Singapore, 1985).
[19] L. D. Landau and E. M. Lifshitz, *Fluid Mechanics*, Course of Theoretical Physics, Vol. 6 (Pergamon, London, 1959).
[20] *Handbook of Mathematical Functions, with Formulas, Graphs and Mathematical Tables*, edited by M. Abramovitz and I. Stegun (Dover, New York, 1965).
[21] One can easily verify that the integral of S_α over all frequencies equals the mean-square value of α.
[22] This step may be rigorously justified since if we introduce the parameter $\xi = \pi am/2R$, the change in ξ from one term to the next is approximately a/R, which is small and tends to zero in the limit $R \to \infty$.
[23] S. Foster, G. A. Cranch, and A. Tikhomirov, Phys. Rev. A **79**, 053802 (2009).
[24] S. Foster, G. Cranch, and A. Tikhomirov, Proc. SPIE **7004**, 70043J (2008).
[25] G. Cranch and S. Foster, Science **335**, 286 (2012).